




## ADAPTATION AND APPLICATION OF A POLARISATION CURVE TEST PROTOCOL FOR A COMMERCIAL PEM ELECTROLYSER ON CELL AND STACK LEVEL

Nicol Daniela JARAMILLO RODRÍGUEZ\*,\*\* , Aline LUXA\*\* , Lars JÜRGENSEN\* 

\*Faculty of Nature and Technology, Energy Technology, Hochschule Bremen, Neustadtswall 30, Bremen, 28199, Germany

\*\*Application Center for Integration of Local Energy Systems ILES,

Fraunhofer Institute for Wind Energy Systems IWES, Am Seedeich 45, Bremerhaven, 27572, Germany

[nrodriguez001@stud.hs-bremen.de](mailto:nrodriguez001@stud.hs-bremen.de), [lars.juergensen@hs-bremen.de](mailto:lars.juergensen@hs-bremen.de), [aline.luxa@iwes.fraunhofer.de](mailto:aline.luxa@iwes.fraunhofer.de)

*received 11 November 2022, revised 2 March 2023, accepted 4 March 2023*

**Abstract:** The present study aims to develop a test protocol based on the literature for electrochemical characterisation of a polymer electrolyte membrane (PEM) electrolysis commercial stack using polarisation curves. For this, a 1-kW water electrolysis test stand with integrated temperature control and measurement systems was built around the stack. Afterwards, the stack performance was characterised under different operating pressure and temperature conditions by using polarisation curves. A measurement protocol was developed based on the literature. To ensure the reproducibility of the results, two rounds of experiments were performed. The experiments were carried out at temperatures between 20 and 60 °C and pressures up to 15 bar. The results show distinct regions in the polarisation curves related to the activation and ohmic overvoltage. The effect of temperature and pressure on the performance is shown and analysed. The performance of single cells in the stack is also measured. The stack polarisation curves are compared with those in the literature, which gives an understanding of the materials used in electrodes and types of membranes.

**Key words:** PEM water electrolysis, test protocol, electrochemical characterisation, polarisation curves

### 1. INTRODUCTION

In the future, green hydrogen is expected to be used as a chemical feedstock for industry and as long-term chemical storage for the energy grid. To support the establishment of the hydrogen market, the German government in the coalition agreement for 2021–2025 proposed an expansion of electrolysis capacity of up to 10 GW in Germany by 2030, based on the National Hydrogen Strategy [1]. Green hydrogen must be produced from renewable energy, which requires high reliability and dynamic capability of electrolyzers [2]. Therefore, the necessary development of the hydrogen economy entails many technical challenges that must be addressed early on for a successful implementation. For polymer electrolyte membrane water electrolysis (PEMWE), the stack is the most expensive component, accounting for about 60 % of the initial costs of an electrolysis plant [3,4]. For this reason, it is important to understand and improve the performance of the stack through electrochemical studies. In this field, one of the most common methods to study electrochemical cells is polarisation curves. These curves show the voltage behaviour of a cell under different current loads at constant temperature and pressure. In addition, a polarisation curve is a tool for comparing between the performance of electrolyzers.

In common data sheets of commercial PEMWE manufacturers, only a system efficiency at nominal load is given. This gives very little information about the stack performance in partial loads. Since polarisation curves cover the whole load range, they can serve as the base for optimising the electrolyser operation. Due to highly fluctuating renewable energy sources, PEMWE may often

have to operate under partial load. Furthermore, in commercial PEMWE plants, condition monitoring is essential to detect or prevent degradation. Polarisation curves can be a powerful tool to track cell degradation. Since high-power PEMWE stacks can have numerous cells, it is complicated to track every single one of them. Moreover, for the PEMWE stack description in modelling, often only the sum of identical single cells is considered for the total stack voltage [5]. However, this does not take account of the ohmic resistance of the end plates. Therefore, it is important to understand the difference and correlation between the polarisation curves of the stack and the individual cell. To the best of the authors' knowledge, there is no generic description of this. It is also necessary to examine the specific ways in which individual cells influence the overall performance of the PEMWE. In addition, the performance of the PEMWE is influenced not only by the power set point but also by temperature and pressure conditions. The effect of these factors has been widely described in the literature [6,7,8]. The findings of single cell examinations should be compared to the influence on a commercial stack on cell and stack level.

The Bremen University of Applied Sciences (HSB) is currently engaged in hydrogen technology research and the implementation of various electrolyser technologies. In this context, the main objective of this work was the electrochemical characterisation of a PEMWE stack using polarisation curves. For this purpose, a 1-kW electrolysis test bench was first set up for educational and research purposes at the Laboratory of Environmental Chemistry of the HSB. Since there is currently no technically standardised and recognised measurement protocol, especially for industrial plants, a suitable protocol was designed from various sources,

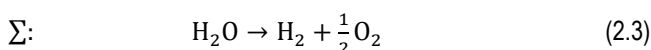
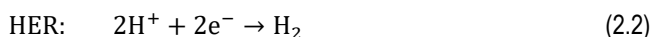
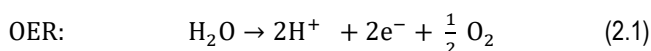
which tested a single cell at the laboratory level [9–11]. For complete characterisation over a wide operating range, experiments were carried out under multiple temperatures and pressures. To monitor the overall performance of the stack, measurements were performed at the stack level and compared with monitoring results of individual cells.

## 2. FUNDAMENTALS

In this chapter, the electrochemical basics are described, which are necessary for the general understanding of the study. Firstly, the redox reaction that occurs during the electrolysis is described, then the voltage necessary for the reaction to occur and the corresponding losses and, finally, the characterisation method, i.e., the polarisation curve.

### 2.1. Polymer electrolyte membrane (PEM) water reaction

In PEMWE, water is split into hydrogen and oxygen by an electrochemical potential. The redox reaction in (2.3) is described by the two half-cell reactions (2.1) and (2.2). The oxygen evolution reaction (OER) takes place at the anode with a required minimum anode potential of 1.23 V, while the hydrogen evolution reaction (HER) takes place at the cathode with a potential of 0 V. Both reactions must be catalysed, and a membrane is located between the electrodes for product separation and for efficient proton transport [12].



During the operation, water flows through the flow field of the bipolar plates, which ensures homogeneous distribution of water over the entire active surface and efficient removal of products from the cell. Within the cell, water flows through the porous transport layer (PTL) on the anode side to the catalyst-coated membrane (CCM), where it is converted into H<sup>+</sup> protons, electrons and oxygen (OER). Oxygen and excess water are transported through the PTL to the anode gas outlet. Electrons leave the anode through the external circuit, providing the driving force (cell voltage). Hydrogen ions move across the membrane to the cathode side, where they recombine with electrons to produce molecular hydrogen (HER). With the increase in current density, the transport of water from the anode to the cathode increases simultaneously due to electroosmotic movement. This entrained water is known as drag water. Hydrogen and drag water are released through the PTL into the flow channels and scrubbed through the cathode gas outlet. The membrane, electrodes and PTLs together form the membrane electrode assembly (MEA). The electrodes are located on both sides of the MEA, and together it is known as the CCM. The designation of CCMs in the literature usually follows this scheme: cathode-catalyst/membrane/anode-catalyst, e.g., Pt/Nafion®-117/IrO<sub>2</sub>, indicating the catalysts (Pt and IrO<sub>2</sub>) used on cathode and anode sides and the membrane (Nafion®-117) in between.

### 2.2. Overvoltage of PEM electrolysis

Previously, the voltage for OER and HER was described for the ideal case. Considering real-time operation, the voltage of an electrolysis cell

$$U_{\text{cell}} = U_{\text{ocv}} + \eta_{\text{act}} + \eta_{\text{ohm}} + \eta_{\text{mass}}, \quad (2.4)$$

can be calculated as the sum of the open-circuit voltage  $U_{\text{ocv}}$  and the losses: the activation overvoltage  $\eta_{\text{act}}$ , ohmic overvoltage  $\eta_{\text{ohm}}$  and mass transport overvoltage  $\eta_{\text{mass}}$ . The percentage of the individual losses depends, to a considerable part, on the design, the materials used and the operating parameters such as pressure and temperature. The open-circuit voltage  $U_{\text{ocv}}$  is the theoretical minimum potential difference between the two electrodes required to start the reaction.

At very low current densities, the total overvoltage is almost entirely determined by the activation overvoltage. The activation overvoltage describes the energy required to initiate the electrochemical reaction. Especially, the OER requires a high activation energy and occurs slower than the HER. The activation surge is directly influenced by temperature, catalyst material and catalyst loading.

The ohmic overvoltage is related to the proton resistance passing through the membrane and the electrical resistance of the components. The proton resistance of the membrane is significant as it is typically 10 times higher than the electrical resistance. With increasing current and proton flow, the ohmic overvoltage also increases linearly. Insufficient humidification of the membrane leads to a decrease in proton conduction, resulting in a higher voltage requirement. Intensified electrical resistance is caused, e.g., by poor contact between the current collectors and the bipolar plates or by passivation of the surfaces through the formation of oxide layers [15]. An increase in membrane thickness also has a negative effect on this overvoltage. However, a thinner membrane could increase the gas permeability [15].

The diffusion or concentration overvoltage refers to transport resistances resulting from insufficient inward transport of water into the stack or of gases and drag water out of the stack. At high current densities, gas bubbles may not be removed from the electrodes as quickly as they are generated. The voltage increases as the active surfaces are covered, the electrical resistance of the cell increases due to the non-conductivity of the bubbles, and the diffusion of water to the active surfaces is restricted.

Increasing the operating temperature of a PEMWE significantly improves the performance of the stack [14]. However, high temperatures increase gas permeability and decrease the mechanical stability of the membrane and may contribute to accelerated degradation [16]. This, along with the stability problems of ion exchange resins at temperatures above 60 °C, is the reason that the temperature in current commercial PEM plants does not usually exceed 60–70 °C [17].

### 2.3. Polarisation-Curve

The polarisation curve shows the relationship between cell voltage and current density, where lower cell potential at higher current density is desirable. It can be used to track cell degradation by comparing the curve at the beginning of life (BoL) and at the end of life (EoL). In addition, a polarisation curve is a

useful and standardised method for comparing the performance of different electrolyzers. During the measurement, constant operating conditions or thermodynamic equilibrium, including temperature and pressure, must be ensured. The polarisation curve can be measured in two ways, under galvanostatic or potentiostatic control. In the first variant, the current density is modified stepwise, while in the second variant, the voltage is changed.

In the following, the polarisation curve of an electrolysis cell is explained and illustrated with the help of Fig. 1. As it can be seen, the cell voltage increases with increasing current density, corresponding to increasing hydrogen production according to Faraday's law. The curve can be roughly divided into three overvoltage dominated ranges, the activation, ohmic, and mass transport range. The area with very low current densities is characterised by a strong voltage rise, which is due to the large influence of the activation overvoltage. Ohmic losses dominate most of the polarisation curve, which is characterised by a linear curve behaviour. With increasing current, a slope change by bending upwards is observed due to mass transport limitation. In this range, the efficiency is low, and the heat dissipation is very high.

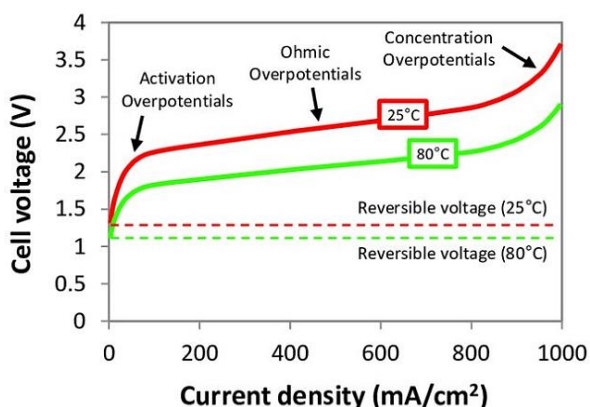


Fig. 1. Typical polarisation curves of an electrolysis cell at two different temperatures [18]

### 3. MATERIALS AND METHODS

For the characterisation process of the PEMWE, a test rig was built around a 1-kW commercial stack. The stack consists of 10 cells connected in series, with an active cell area of 30 cm<sup>2</sup> each. The characteristics of the stack according to the manufacturer are listed in Tab. 1. Details of the PEM cell materials are confidential by the commercial stack manufacturer and have not been provided to the stack owner.

The pressures referred to in this article are measured above atmospheric pressure and are expressed in units of bar. The stack operates under differential pressure, where the pressure on the cathode side can reach up to 20 bar, while the maximum allowable pressure on the anode side is limited to 0.5 bar. According to the manufacturer, a water inflow of 66 l/h at the anode side is needed to ensure a maximum temperature difference

$$\Delta T_s = T_{in,anode} - T_{out,anode}, \quad (3.1)$$

between the inlet and the outlet temperature of the

ode  $\Delta T_s$  of 10 K. While most of the water is used for cooling the stack, only a small amount is required for the reaction. Moreover, drag water is carried to the cathode side through the membrane, which is about 1 l per standard cubic meter of produced hydrogen.

Tab. 1. PEM stack technical specifications

Feature	Value	Unit	Feature	Value	Unit
Temperature $T_{in,anode}$	20–70	°C	Cells	10	-
Max. $\Delta T_s$	10	K	Active area	30	cm <sup>2</sup>
Max. voltage	25	V	O <sub>2</sub> operating pressure	<0.5	bar
Minimal current	15	A	H <sub>2</sub> operating pressure	Max 20	bar
Nominal current	52.5	A	H <sub>2</sub> O conductivity	0.1	μS/cm
Max. current	75	A	Cooling water flow rate	66	l/h
Nominal power	1	kW	H <sub>2</sub> O consumption	1	kg/h
Min. power	0.25	kW	$\eta_{nominal}$	78	%
Max. power	1.88	kW	H <sub>2</sub> -production	0.06 to 0.31	m <sup>3</sup> /h @STP

PEM, polymer electrolyte membrane

To operate the stack, the following subsystems have been installed: process water loop, stack power supply, thermal management, hydrogen production subsystem, nitrogen inertisation subsystem, measurement subsystem and a central data acquisition subsystem. In the following text, the systems mentioned are described with the help of the flow diagram in Figs. 2 and 3, which shows the setup in the laboratory. The process water circuit operates on the anode side. First, there is a peristaltic pump (P-1) to ensure a constant flow of water through the stack. Downstream, there are two counterflow glass heat exchangers (W- 1 and W-2). To operate the PEMWE, the conductivity of water must be less than 0.1 μS/cm. This is achieved with an ion exchange resin bed (F-2), which separates harmful metal ions and measured with a conductivity sensor (QI-1) placed in a parallel pipe. A filter (F-3) is used upstream of the stack and downstream of the ion exchanger to prevent contaminant particles coming into the stack, such as resin, that can be released from the ion exchanger. After the stack, the water with the produced oxygen flows to the oxygen tank (F-1), where gas and liquid are separated by gravity. To compensate for the water consumed by losses from the water splitting reaction, water can be added to the system through the oxygen tank. Water is added on the anode side because it is needed for OER, and the oxygen tank is not overpressurised. Two temperature sensors (TIRC-2 and TIR-3) are placed to measure the inlet  $T_{in,anode}$  and outlet water temperature of the stack  $T_{out,anode}$ . The sensors are used to record the temperature difference of the stack  $\Delta T_s$  (TDIC-1).

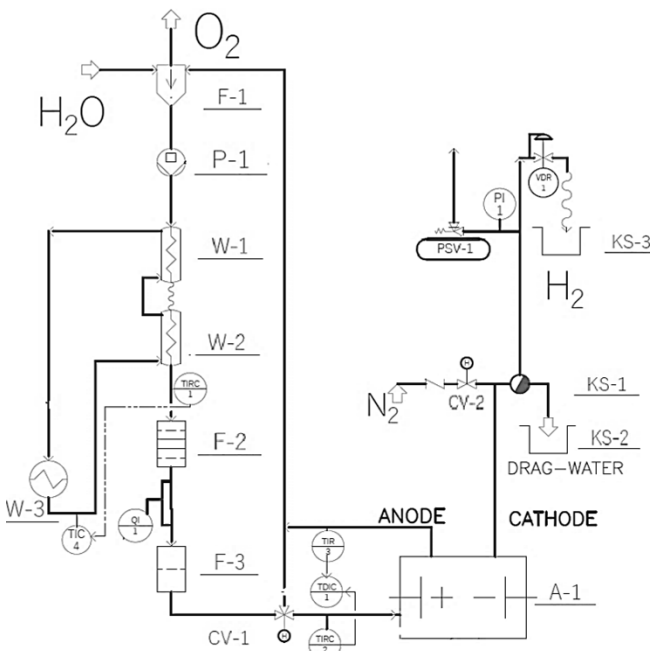


Fig. 2. Piping and instrument flow diagram of the test rig

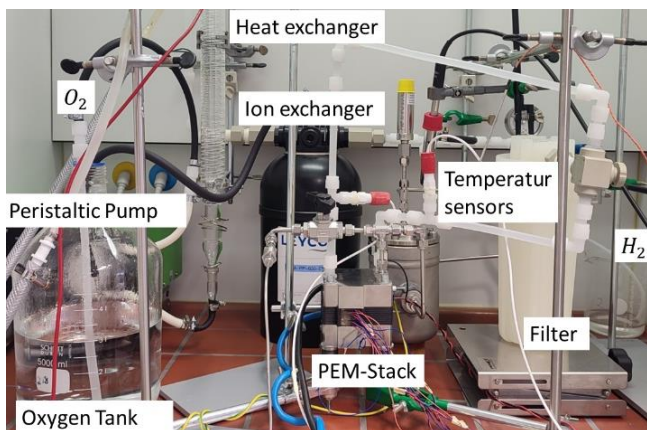


Fig. 3. Installed test bench for PEM electrolysis with 1 kW nominal power

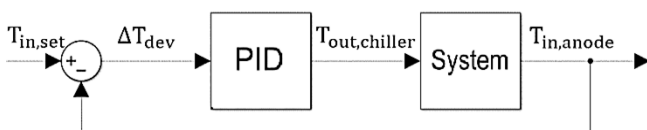


Fig. 4. Schematic of the stack anode inlet temperature control loop by means of the internal PID of the chiller.

For temperature regulation, a chiller (W-3) is connected to the heat exchangers and used to control the process water temperature feeding the stack  $T_{in,anode}$ . The temperature signal from the sensor before the stack is compared with the reference temperature  $T_{in,set}$ . According to the control error  $\Delta T_{dev}$ , the chiller regulates its water outlet temperature  $T_{out,chiller}$  by its internal proportional–integral–derivative (PID) controller. A schematic of the temperature control is shown in Fig. 4. This allows automatic regulation of the stack supply temperature. A proportional–integral (PI) controller would probably be sufficient, but the chiller with its PID was available in the laboratory for use.

The produced gases leave the stack (A-1) mixed with liquid

and gaseous water. In this system, liquid water is separated on the cathode side using a ball float steam trap (KS-1). A pre-pressure regulator (VDR-1) is installed to maintain the pressure in the system. Additionally, a safety valve (PSV-1) is placed upstream of the pressure regulator, which opens if the system pressure exceeds 18 bar, to ensure that the maximum pressure is not reached on the cathode side of the stack. The pressure is also monitored and displayed by a pressure gauge (PI-1). The inertisation subsystem is connected to the cathode side of the stack. Nitrogen is used as an inert gas for the inertisation of the hydrogen pipes and components.

To operate the stack, software of the power supply is used, in which it is possible to program what current or voltage the stack receives. To protect the stack from high voltages, the power supply is programmed to a cut-off voltage of 25 V according to the manufacturer’s specifications. Current and voltage measurements of the stack are also carried out by the power supply. Noise and impedance effects have been minimised with the addition of two twisted sense wires as recommended in the power supply manual. In addition to data collection by the power supply, a data acquisition program was developed in LabVIEW [19] to measure the temperature of the process water loop and voltage of the single cells. The individual cells were measured by attaching cables directly to the contacts of each cell and then the cables were connected to a National Instruments Module 9215. This way, the individual cells can be monitored, and short circuits between individual cells can be detected.

The measurement protocol for polarisation curves was also developed. The protocol can be used on all commercial electrolyzers, which can be installed on the test rig setup in this study. In general, it can be adapted to other test rigs, but there may be limitations that need to be considered such as temperature and flow rate.

The polarisation curves have been recorded under galvanostatic control. According to Ref [11], the cell voltage should not deviate by more than  $\pm 5$  mV during a 30-s period. For this reason, each step of the current density should last at least 30 s. To verify that the system is in thermodynamic equilibrium, two polarisation curves are recorded for each experiment. At atmospheric pressure, the ascending polarisation curve is first determined, i.e., the lowest allowable current is applied to the stack. The current is gradually increased until the maximum value of 75 A ( $2.5 \text{ A/cm}^2$ ) is reached. Then, the descending polarisation curve is recorded from the highest current to the lowest current. Under pressure, the process is reversed. If the curves strongly deviate from each other, this speaks of hysteresis and thus of a system that is not in equilibrium, and the experiment must be repeated [11]. Furthermore, each experiment was performed twice to ensure reproducibility of the measurement results.

The larger the current range over which the polarisation curve is taken, the more the information about a wide operating range of the stack is obtained. However, the lower part of the load range is limited by hydrogen permeation to the anode, which increases at low operating current densities [20], while at the upper part of the load range, a maximum current given by the manufacturer is the technical limiting aspect. The minimum current recommended by the manufacturer, that is applied to the PEMWE, is 15 A respectively  $0.5 \text{ A/cm}^2$ . To obtain more information about the activation losses of the stack, lower currents from  $0.006 \text{ A/cm}^2$  (0.2 A) were used with the low current density steps lasting



only 399 s, instead of the suggested 30 s due to safety aspects. The shorter steps avoid excessive hydrogen concentration on the anode side, which could lead to recombination of hydrogen with oxygen and thus could lead to a rupture of the membrane. The polarisation curve data acquisition is divided into three parts, which can be seen in Tab. 2. This table shows the current steps for each section and the duration of each step. It has been found in the literature that no mass transport losses are observed in

some commercial electrolysers even at 5 A/cm<sup>2</sup> [14]. However, depending on the design, mass transport losses can occur earlier. Therefore, several steps are initially performed in the range of 2–2.5 A/cm<sup>2</sup>. After no mass transport losses have been observed in the first experiments, the same step size as in the ohmic loss range is maintained. The current steps applied do not exceed the maximum current ramp of 5 A/s, as specified by the stack manufacturer.

**Tab. 2.** Operating procedure for recording of polarisation curves at atmospheric pressure. For 5 bar, 10 bar, and 15 bar, the data acquisition steps for the polarisation curves were performed in the reverse order

Step	Description	Details
Warm up	Start the system, set the temperature and wait until the operating conditions stabilise	(1) H <sub>2</sub> O conductivity 0.1 μS/cm (2) Pump volume flow 160 l/h (3) Stack inlet temperature 20 °C, 30 °C, 40 °C, 50 °C, 60 °C (4) Overpressure at the cathode 0, 5 bar, 10 bar, 15 bar
Data acquisition (polarisation curve)	Conduct current-controlled polarisation curves at constant temperature and pressure	(1) Ascending curve <ul style="list-style-type: none"> <li>• Activation overvoltage 1 <ul style="list-style-type: none"> <li>○ Step size: 0.025 A/cm<sup>2</sup></li> <li>○ Range: 0.006–0.15 A/cm<sup>2</sup></li> <li>○ Step duration: 5 s</li> </ul> </li> <li>• Activation overvoltage 2 <ul style="list-style-type: none"> <li>○ Step size: 0.05 A/cm<sup>2</sup></li> <li>○ Range: 0.2–0.5 A/cm<sup>2</sup></li> <li>○ Step duration: 30 s</li> </ul> </li> <li>• Ohmic overvoltage <ul style="list-style-type: none"> <li>○ Step size: 0.1 A/cm<sup>2</sup></li> <li>○ Range: 0.6–2.5 A/cm<sup>2</sup></li> <li>○ Step duration: 30 s</li> </ul> </li> </ul> (2) Descending curve with the same steps
Shutdown	Prepare the system for the shutdown under security precautions	1) Turn off the power supply 2) Ensure water flow through the stack for a further 5 min 3) Open the nitrogen valve for purge

For each test, the temperature and pressure in the stack are kept constant during data acquisition. As the safety valve is set at 18 bar, pressures of 0 bar, 5 bar, 10 bar, and 15 bar are used on the cathode side, and the anode is not pressurised. The operation temperature is limited by the maximum operating temperature of the ion exchanger, which is 60 °C. For this reason, the experiments are carried out at five stack inlet temperatures: 20 °C, 30 °C, 40 °C, 50 °C, and 60 °C. For reliable results, the temperature difference in the stack  $\Delta T_s$  should be as small as possible, and the stack supply temperature  $T_{in,anode}$  should be kept constant [11]. According to this, the flow rate of the pump is maintained at the maximum of 160 l/h for all experiments, allowing a temperature difference  $\Delta T_s$  of less than  $\pm 5$  K. This is below the  $\pm 10$  K limit specified by the manufacturer but higher than  $\pm 2$  K, which is recommended by other reports [9–11]. In this work,  $\Delta T_{dev}$  is defined as follows:

$$\Delta T_{dev} = T_{in,set} - T_{in,anode} \leq \pm 2 \text{ K} \quad (3.2)$$

A deviation of  $\pm 2$  K from the inlet temperature set ue  $T_{in,anode}$  was tolerated.

#### 4. RESULTS AND DISCUSSION

The results are obtained from the polarisation curves of 7 of the 10 single cells and the entire stack, as well as the

temperatures and pressures in the system during the 32 experiments. The influence of the operating factors, temperature and pressure is shown by the polarisation curves. Since the cells are connected in series, the sum of the cell voltage should amount to the total stack voltage. Therefore, to compare the performance of the entire stack with the performance of the individual cells, the total voltage measured by the power supply is divided by the number of cells.

Fig. 5a shows the current density and voltage during an experiment at 60 °C and 5 bar. The decreasing current density steps are shown in red, and the resulting stack voltage is shown in green. Fig. 5b shows the behaviour of the inlet and the outlet temperature of the stack, as well as the temperature difference. The inlet temperature of the stack  $T_{in,anode}$  remains almost constant and is independent of the current. It remained below the permitted value deviation of the set inlet temperature of  $\pm 2$  K in this experiment as well as in all other experiments. The outlet temperature of the stack decreases until a current density of about 0.6 A/cm<sup>2</sup> (18 A) is reached. After that, the outlet temperature remains almost the same as the inlet temperature. The temperature difference in this experiment decreases from about 4 K to about 0 K from the highest current density of 2.5–0.6 A/cm<sup>2</sup>. Then, it remains almost constant at  $-0.25$  K until the lowest current density is reached. The temperature difference  $\Delta T_s$  remains within the permissible range of  $\pm 5$  K throughout all experiments.

The stack responds quickly to a current variation, with the

voltage value adjusting within 2 s of a change in current. Therefore, 30 s at each current density step was sufficient to guarantee the maximum variation of 5 mV. No significant hysteresis was observed in any of the experiments, indicating that the system was in thermodynamic equilibrium during all measurements, which can be seen in Fig. 9 of the Appendix. Furthermore, the feasibility of the experiment is proven with a second set of experiments. A minimal difference was found between the first and second series of tests, with the largest difference being 0.022 A/cm<sup>2</sup>, seen in the polarisation curve at 30 °C and 0 bar at maximum current density. The results can be seen in Fig. 10 of the Appendix.

In general, all the polarisation curves taken show two zones that are related to the activation and ohmic losses. From 0 to about 0.2 A/cm<sup>2</sup>, the polarisation curve has a behaviour analogous to the Butler-Volmer equation from Ref [14] used to describe the activation overvoltage, which is of the form  $\sinh^{-1}(x)$ . At approximately 0.2 A/cm<sup>2</sup>, the polarisation curve behaves linearly with increasing current density up to the maximum current density of 2.5 A/cm<sup>2</sup>. It can also be seen that most of the curve has a linear behaviour, i.e., the ohmic losses dominate most of the polarisation curve. As mentioned in Section 2.3, an exponential increase in voltage is expected at higher current densities due to the mass transport limitation. This behaviour was not observed up to current densities of 2.5 A/cm<sup>2</sup>, which also has been found in other studies [9,14,6]. Accurate identification of the precise limits of the loss regions requires further studies such as electrochemical impedance spectroscopy (EIS) [21].

#### 4.1 Effect of operating temperature and pressure

In this paragraph, the effect of the operating conditions on the stack performance are described. Fig. 6a shows the influence of temperature on the polarisation curve of the stack at a constant pressure of 0 bar. The polarisation curve is strongly dependent on the operating temperature. At a current density of 2.5 A/cm<sup>2</sup>, the voltage of the stack increases by 14 % when the temperature rises from 20 °C to 60 °C. The black square in Fig. 6a represents the nominal voltage efficiency  $\eta_V$  of the stack of 78% (1.48 V/1.90 V) at a nominal current density of 1.75 A/cm<sup>2</sup> according to the manufacturer. This point is closer to the polarisation curve of 60 °C.

In the first part of the polarisation curve from 0 to about 0.2 A/cm<sup>2</sup>, the curves differ slightly from each other, showing an influence of temperature on the voltage; however, it is small compared to the rest of the curve. At a constant current density of 0.2 A/cm<sup>2</sup>, the highest voltage difference is 31 mV between the temperatures of 20 °C and 30 °C. The smallest difference at the same current density is 19 mV and was found between the 50 °C and 60 °C curves. In the second part of the curve, from 0.2 A/cm<sup>2</sup> to 2.5 A/cm<sup>2</sup>, the voltage difference between the curves begins to increase linearly at different temperatures. At a current density of 2.5 A/cm<sup>2</sup>, the largest voltage difference is 108 mV, also between 20 °C and 30 °C.

The results indicate that the stack voltage decreases as the temperature increases, which brings the cell voltage closer to the thermoneutral voltage. This confirms that the electrolysers have better performance at higher temperatures. The reason for this could be the higher ionic conductivity of the membrane at higher temperatures, leading to lower ohmic losses. This is observed since the results showed a higher slope of the curve at 20 °C than the slope of the curve at 60 °C in the linear range of the polarisation curve. In addition, higher temperatures could also facilitate faster reaction kinetics, resulting in lower kinetic overvoltage. As shown in the small box in Fig. 6a, electrolysis starts faster at higher temperatures, indicating that the activation barrier is lower at higher temperatures. Another effect that may influence this behaviour is the dependence of the open-circuit voltage on temperature. At the lowest tested current density of 0.006 A/cm<sup>2</sup>, voltages of about 1.490 V at 20 °C and 1.433 V at 60 °C have been measured. The experiment that came closest to the thermoneutral voltage at standard conditions was the polarisation curve at 20 °C and atmospheric pressure. The slightly lower starting voltage at high temperatures can be explained by the partial pressure of the water vapour in the catalytic interface region of the electrolyte, and the same behaviour was observed in another test setup [6].

The polarisation curves of the 10-cell stack at different cathode pressures are shown in Fig. 6b. The voltage increases with increasing pressure at all current densities, which means that the performance of the stack decreases at higher pressure; however, this is not particularly dominant. The influence of pressure on the polarisation curve of the stack was mainly observed in the activation zone. With increasing current density, the pressure has barely any effect due to the lack of correlation between the pressure and ohmic resistance of the membrane, as described in the study in Ref [14]. For 2.5 A/cm<sup>2</sup>, the difference is about 13 mV between 0 bar and 15 bar.

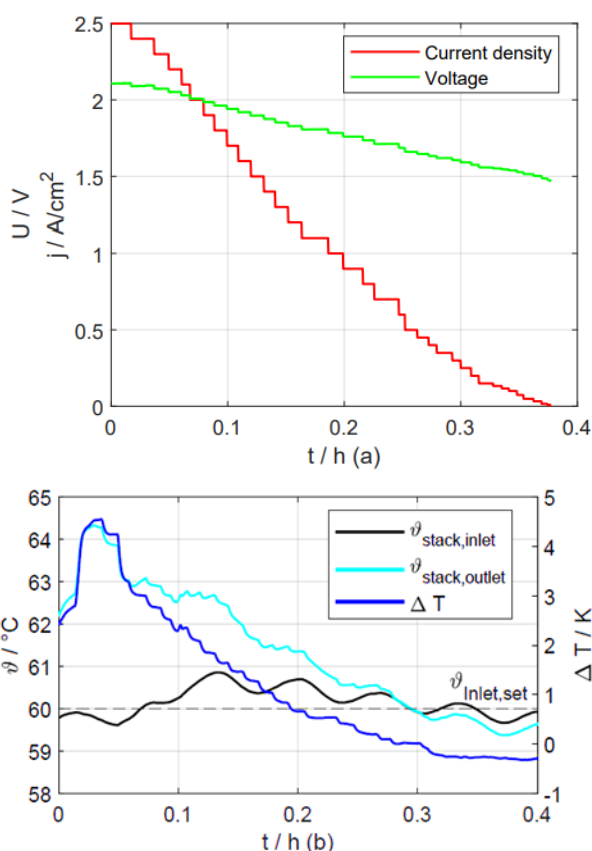


**Fig. 5.** (a) Current density steps and voltage for the polarisation curves, at 60 °C and 5 bar with decreasing current density (b) Course of the inlet and the outlet temperature as well as the temperature difference in the stack

### 4.2 Single cell measurements

Measurements were made in 7 out of 10 cells, as three of them could not be considered due to measurement errors. Fig. 7 shows the polarisation curves at 40 °C and 15 bar pressure. For the other tested temperatures and pressures, a similar behaviour as in Fig. 7 was observed.

The performance of the cells is generally similar at all current densities. At low current densities between 0 A/cm<sup>2</sup> and 0.5 A/cm<sup>2</sup>, in the overvoltage activation zone, the polarisation curves are almost overlapping and show a negligible difference. From this, it could be concluded that all cells have the same catalysts with the same loads and that the catalyst is applied homogeneously over the entire electrode. From about 0.5 A/cm<sup>2</sup>, where the linear region of the polarisation curve begins, the polarisation curve of the cells and of the stack start to diverge from each other as the current density increases. This may be due to the cells and the stack having different ohmic losses. Ohmic losses may differ between cells because of different electric contacts between the cells. Currently, electrolysis stacks are mostly produced manually, which can lead to inhomogeneities during the series connection or stacking of cells. The order of the cells at 2.5 A/cm<sup>2</sup> from best to lowest performance is 3, 6, 7, 8, 2, 10, and 4. Additionally, the stack always has higher voltage values than the cells.

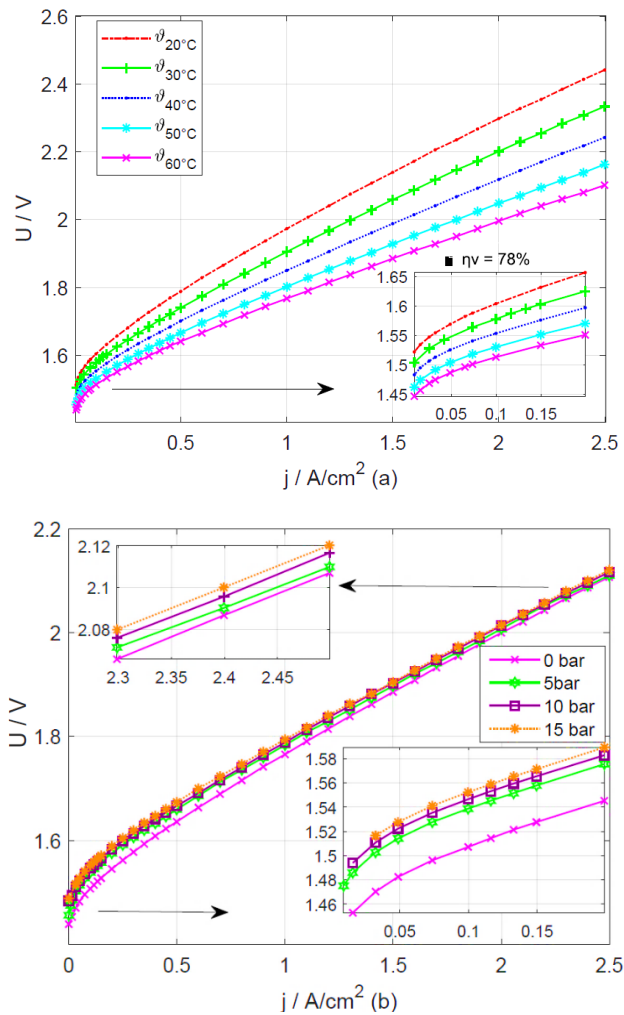


Fig. 6. (a) Effect of temperature on the performance of the stack at a constant pressure of 0 bar. (b) Effect of pressure on the performance of the stack at a constant temperature of 60 °C

The ohmic losses of the stack are higher than those of the cells since the stack measurement also considered the end plates, while the measurement of the cells was directly performed at the cell electrodes. Furthermore, as pressure increases, the voltage difference between the cells tends to widen, which is expected as high pressure can lead to reduction in the contact area. In particular, the cells far from the water inlet (e.g., cell 10) showed higher voltage at high currents than the first cells (e.g., cell 3). This may mean that irregular water distribution or more difficult gas removal may occur in the cells far from the water inlet. Since no clear mass transport losses are observed in general, this is unclear. Cell 4 shows the highest voltage values, which is inconsistent with the assumption of transport losses mentioned earlier. In this case, the explanation could be that in the middle part of the stack, the contact resistance between the membrane and the electrodes, as well as that between the bipolar plates and the CCMs, increases due to less compression of the cells.

However, it is important to note that the cells are generally very close to each other at all current densities, and the largest voltage difference is between the cells and the stack. In this study, the difference recorded between the cells is not considerable, as mentioned in the study in Ref [6]. It was found that improper contacts lead to uneven current distribution and a higher operating voltage to compensate for the non-active zones [6]. As high voltages were not seen in this work, it can be assumed that the CCMs of the stack have good contact with the bipolar plates and the cells to each other. However, in Ref [6], it was found that the effects of contact areas on stack performance at higher current densities were more pronounced, which could be an explanation for why the cell curves are further apart at current densities above 2 A/cm<sup>2</sup>.

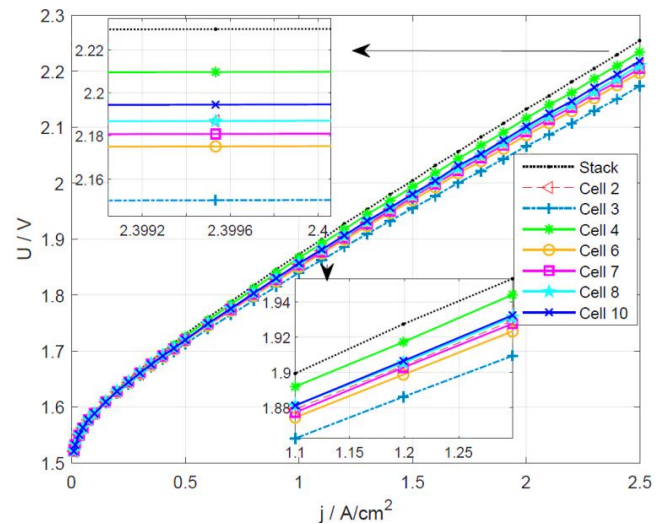
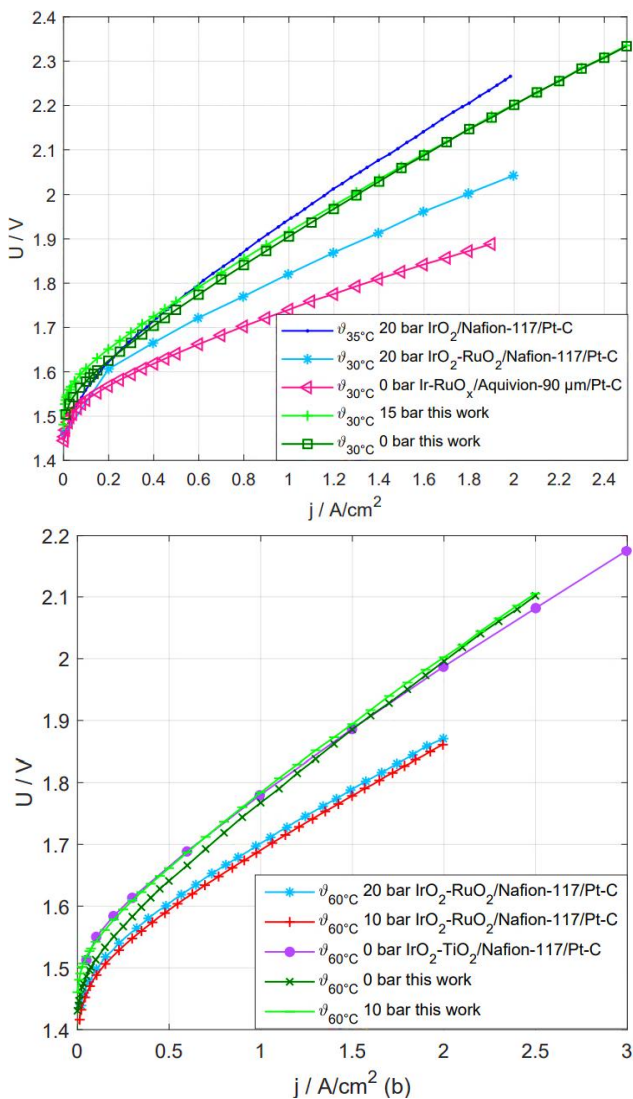


Fig. 7. Polarisation curve at 40 °C and 15 bar. Visualisation of the behaviour of the stack and 7 cells

### 4.3 Comparison with other PEM electrolysis systems

In this section, the experimental data obtained in this study are compared with those of four studies. It should be noted that the specific materials used in the PEMWE for this study were not disclosed by the commercial stack manufacturer and were not made available to the authors. Since the composition of the CCM of the stack used in this work is not known, it is of interest to the

authors for research purposes to draw general assumptions about the materials used in the commercial stack, through comparisons with the performance of other cells. Moreover, it should be noted that the polarisation lines of the present study shown in this section are from the stack, while all those in the literature are from a single cell since characterisation and fabrication of a single cell are generally easier.



**Fig. 8.** (a) Comparison of polarisation curves from this work and the literature in the temperature range of 30 °C and 35 °C and pressure range of 0 bar and 20 bar [2,23]. (b) Comparison of polarisation curves from this work and the literature at 60 °C and pressure range of 0 bar and 20 bar [17,22]

Fig. 8a illustrates the results presented in Ref [22] for temperatures near 30 °C and pressures of 0 bar and 20 bar, with the dark blue being a IrO<sub>2</sub>/Nafion®-117/Pt-C and the light blue an IrO<sub>2</sub>-RuO<sub>2</sub>/Nafion-117/Pt-C cell. The polarisation curve at 0 bar with a 90-µm-thick Aquivion® membrane with IrRuO<sub>x</sub> and Pt/C catalysts deposited on both sides of the membrane is shown in pink [23]. For comparison, the polarisation lines of this work closest to the operating conditions of the other works are also plotted in Fig. 8a. The polarisation curve at 35 °C and 20 bar with a IrO<sub>2</sub>/Nafion-117/Pt-C cell is the curve closest to the values of the investigated stack at 30 °C. It can also be noted that the other two

curves (pink and light blue) are far from the results obtained here. These show lower voltage values at the same current density, i.e., better performance. These two curves use a RuO<sub>x</sub> catalyst on the anode side. It has been found in the literature that the use of RuO<sub>x</sub> improves the rate of the OER. Although RuO<sub>x</sub> has a much lower overvoltage than other electrocatalysts in the OER, RuO<sub>x</sub> dissolves and becomes corroded at a higher rate during oxygen evolution [16]. This could be a reason why electrolyser manufacturers use IrO<sub>2</sub> instead of RuO<sub>x</sub> [14]. In addition, the Aquivion® membrane is thinner (90 µm) than that of Nafion® 117 (175 µm), which reduces ohmic losses.

Fig. 8b illustrates the results presented in Ref [22] at 60 °C and at pressures ranging from atmospheric to 20 bar. The polarisation curves from the study [22] are shown in blue for 20 bar and in red for 10 bar. The results from the present study at 10 bar are shown in light green, and the results at 0 bar are shown in dark green. A polarisation curve for a CCM with a Nafion®-117 membrane and a catalyst on the anode of IrO<sub>2</sub>/TiO<sub>2</sub> and Pt/C on the cathode from the study in Ref [17] at 60 °C and ambient pressure can also be found in purple. This polarisation curve is very close to the curve measured in this work at 60 °C and 10 bar. It could be assumed that the performance of the used commercial stack is close to that of a cell with IrO<sub>2</sub>/TiO<sub>2</sub> electrodes and a Nafion®-117 membrane. However, other factors of the stack design that affect the cell's performance must be considered such as the influence of ionomer content, catalyst loading, membrane wetting and other factors [17].

In the study in Ref [17], it was found that the cell voltage difference between 40 °C and 80 °C is about 160 mV at a current density of 1 A/cm² and increases to more than 250 mV at 3 A/cm². In the present study, a voltage difference of 212 mV was measured between 20 °C and 60 °C at a current density of 1 A/cm² and at 2.5 A/cm², the voltage difference increases to 397 mV. In [17] it was pointed out that this difference is due to a 50 % increase in membrane conductivity between 40 °C and 80 °C. In all the polarisation curves shown in this article, measured up to 3 A/cm², no mass transport overvoltage is visible.

## 5. CONCLUSIONS

A 1-kW water electrolysis test stand was set up at the Bremen University of Applied Sciences for hydrogen production. The electrochemical characterisation of the stack and the cells was realised using the polarisation curves. A galvanostatic control was used to characterise up to 2.5 A/cm², at 5 different temperatures of 20 °C, 30 °C, 40 °C, 50 °C, and 60 °C and at 4 different pressures of 0 bar, 5 bar, 10 bar, and 15 bar. The developed protocol for data collection was explained and can be used in future experiments. This work has shown that temperature is the most significant factor influencing the performance of the stack. Increasing the pressure also affects the stack performance, although by a lower percentage. High temperature and atmospheric pressure on the cathode side were found to be the most favourable operating conditions for best efficiency. However, the operation of the stack at higher pressures allows the production of pressurised hydrogen without severely affecting the performance on the stack level. Two zones of stack operation were also identified, one is dominated by activation voltage losses and the other is dominated by ohmic losses. No significant mass transport losses were found.



The stack has a higher voltage than the group of single cells due to its higher ohmic losses. It has also been found that not all cells have the same voltage value, especially in the area where ohmic losses dominate. However, the cells are generally very close together at all current densities. It could be assumed that the membranes of the stack have good contact with their catalyst layers, which also applies to the current collector with the bipolar plates and between them. In addition, it has been found not to be suitable to describe the total stack voltage by the sum of  $N$  identical individual cells. This is especially important for modelling and scaling of electrolyzers based on single cell tests. The comparison of the results of this work with those from the literature showed that the performance of the stack from this work is comparable to that of an IrO<sub>2</sub>-TiO<sub>2</sub> Nafion-117/Pt-C cell. However, this cannot be assured with the present results.

In future work, the parameters of an existing electrochemical model of the stack will be determined using the experimental data from this work. These electrochemical parameters will be integrated into a MATLAB-Simulink® model to simulate the stack and the complete system as part of the Hydrogen Lab Bremerhaven of the Fraunhofer Institute for Wind Energy Systems (IWES). In addition, the experimental data obtained in this work can be used to validate the modelling of the stack. Furthermore, it is desired to identify the percentage of voltage losses due to the end plates.

## 6 APPENDIX

The hysteresis was taken in all experiments, and in this section, the largest hysteresis is shown, which has been measured at 60 °C and 0 bar. In Fig. 10, the comparison between the first and the second round of experiments at 0 bar and at 4 different temperatures 30 °C, 40 °C, 50 °C, and 60 °C is given. The other experiments at 5 bar, 10 bar and 15 bar have a similar behaviour to the experiment presented in Fig. 10.

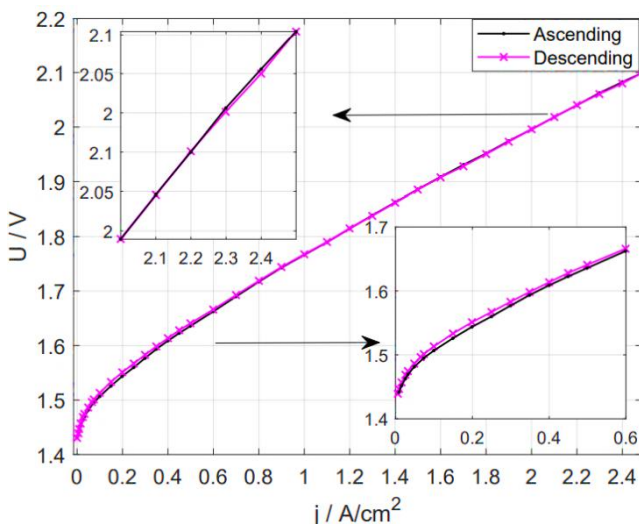


Fig. 9. Hysteresis at 60 °C and 0 bar

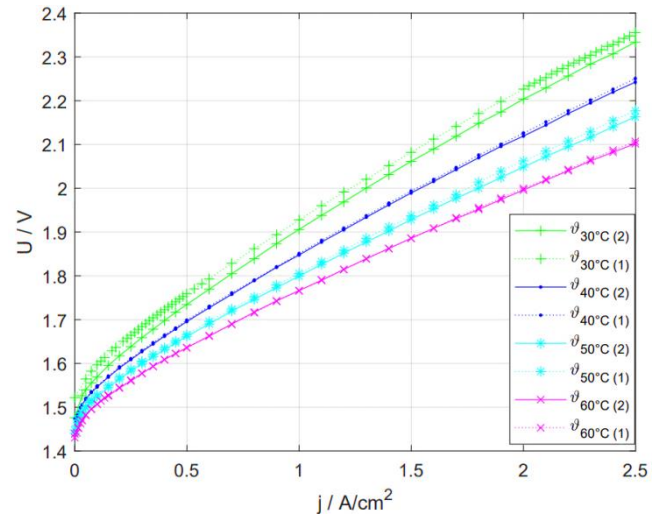


Fig. 10. Comparison between the first and second round of experiments at different temperatures and a constant pressure of 0 bar

## REFERENCES

1. Der Sozialdemokratischen Partei Deutschlands (SPD). BÜNDNIS 90/DIE GRÜNEN und den Freien Demokraten, Koalitionsvertrag 2021 – 2025: mehr fortschritt wagen Bündnis für Freiheit Gerechtigkeit und Nachhaltigkeit. 2021
2. European Commission. Hydrogen: The EU's hydrogen strategy explores the potential for renewable hydrogen to help decarbonise the EU in a cost-effective way [Internet]. 2022 [cited 2022 Nov 06]; Available from: [https://ec.europa.eu/info/index\\_en](https://ec.europa.eu/info/index_en)
3. Bertuccioli L, Chan A, Hart D, Lehner F, Madden B, Standen E. Study on development of water electrolysis in the EU: Fuel Cells and hydrogen Joint Undertaking. 2014
4. Lettenmeier P. Entwicklung und Integration neuartiger Komponenten für Polymerelektrolytmembran- (PEM) Elektrolyseure [PhD Dissertation]. Stuttgart: Fakultät Energie-, Verfahrens- und Biotechnik der Universität Stuttgart. 2018
5. Abomazid AM, El-Taweel NA, Farag HEZ. Novel Analytical Approach for Parameters Identification of PEM Electrolyzer. IEEE Transactions on Industrial Informatics. Sept. 2022; 18(9): 5870-5881. doi: 10.1109/TII.2021.3132941
6. Selamet ÖF, Acar MC, Mat MD, Kaplan Y. Effects of operating parameters on the performance of a high-pressure proton exchange membrane electrolyzer. Int. J. Energy Res. 2013; 37: 457-467. <https://doi.org/10.1002/er.2942>
7. Smolinka T, Ojong E, Garcke J. Hydrogen Production from Renewable Energies—Electrolyzer Technologies. Electrochemical Energy Storage for Renewable Sources and Grid Balancing. Elsevier; 2015. DOI 10.1016/B978-0-444-62616-5.00008-5.
8. Tjarks G. H, Stolten D, Wessling M. PEM-Elektrolyse-Systeme zur Anwendung in Power-to-Gas Anlagen. Forschungszentrum Julich GmbH, Zentralbibliothek (Schriften des Forschungszentrums Julich / Reihe Energie & Umwelt: Reihe Energie & Umwelt). 2017. – ISBN 9783958062177
9. Bender G, Carmo M, Smolinka T, Gago A, Danilovic N, Mueller M, Ganci F, Fallisch A, Lettenmeier P, Friedrich K A, Ayers K, Pivovar B, Mergel J, Stolten D. Initial approaches in benchmarking and round robin testing for proton exchange membrane water electrolyzers. International Journal of Hydrogen Energy. 2019; 44: 9174-9187. <https://doi.org/10.1016/j.ijhydene.2019.02.074>
10. European European Commission, Joint Research Centre, Tsotridis G, Pilenga A. EU harmonized protocols for testing of low temperature water electrolysis. Publications Office of the European Union; 2021. Available from: [doi/10.2760/58880](https://doi.org/10.2760/58880)

11. Malkow T, Pilenga A, Tsoitridis G, De Marco G. EU harmonised polarisation curve test method for low-temperature water electrolysis. Publications Office of the European Union; 2018. Available from: doi:10.2760/179509
12. Godula-Jopek, A. Hydrogen production By electrolysis. Weinheim: Wiley-VCH-Verl., 2015
13. Mori M, Mržljak T, Drobnič B, Sekavčnik M. Integral Characteristics of Hydrogen Production in Alkaline Electrolysers. *Strojinski Vestnik*. Aug 2013; 59(10):585-594. doi: 10.5545/sv-jme.2012.858
14. Espinosa-López M, Darras C, Poggi P, Glises R, Baucour P, Raktondrainibe A, Besse S, Serre-Combe P. Modelling and experimental validation of a 46 kW PEM high pressure water electrolyzer. *Renewable Energy*. 2018; 119: 160–173. <https://doi.org/10.1016/j.renene.2017.11.081>
15. Bensmann, B. Systemanalyse der Druckwasser-Elektrolyse im Kontext [PhD Dissertation]. Magdeburg: Fakultät für Verfahrens- und Systemtechnik der Otto-von-Guericke-Universität Magdeburg. 2017
16. Feng Q, Yuan X, Liu G, Wei B, Zhang Z, Li H, Wang H. A review of proton exchange membrane water electrolysis on degradation mechanisms and mitigation strategies. *Journal of Power Sources*. 2017; 366: 33–55. <https://doi.org/10.1016/j.jpowsour.2017.09.006>
17. Bernt M. Analysis of Voltage Losses and Degradation Phenomena in PEM Water Electrolyzers [PhD Dissertation]. Munich: Fakultät für Chemie der Technischen Universität München. 2018
18. Amores E, Rodríguez J, Oviedo, Lucas-Consuegra A. Development of an operation strategy for hydrogen production using solar PV energy based on fluid dynamic aspects. *Open Engineering*. 2017; 7(1): 41–152. doi: 10.1515/eng-2017-0020
19. Bitter R, Mohiuddin T, Nawrocki M. LabVIEW: Advanced programming techniques. Crc Press; 2006
20. Stähler M, Stähler A, Scheepers F, Carmo M, Lehnert W, Stolten D. Impact of porous transport layer compression on hydrogen permeation. *PEM water electrolysis*. 2020; 45(7): 4008-4014.
21. Merwe J. Characterisation of a proton exchange membrane electrolyser using electrochemical impedance spectroscopy [PhD Dissertation]. Potchefstroom: School of Electrical, Electronic and Computer Engineering North-West University. 2012
22. Bessarabov D, Millet P. PEM Water Electrolysis [Internet]. 1th ed. Elsevier; 2018. Chapter 2, Key Performance Indicators; [cited 2022 Sep 30]. pp. 33–60. Available from: <https://www.elsevier.com/books/pem-water-electrolysis/pollet/978-0-08-102830-8>
23. Siracusano S, Trocino S, Briguglio N, Baglio V, Aricò AS. Electrochemical Impedance Spectroscopy as a Diagnostic Tool in Polymer Electrolyte Membrane Electrolysis. *Materials (Basel)*. 2018; 11(8):1368. doi: 10.3390/ma11081368

This work was partly supported by the Free and Hanseatic City of Hamburg.

Nicol D. Jaramillo Rodríguez:  <https://orcid.org/0000-0002-0745-8642>

Aline Luxa:  <https://orcid.org/0000-0002-3025-3274>

Lars Jürgensen:  <https://orcid.org/0000-0002-7742-8051>



This work is licensed under the Creative Commons BY-NC-ND 4.0 license.